J Mater Sci (2008) 43:6144–6158
DOI 10.1007/s10853-008-2935-0

A critical assessment of the methods for intercalating anionic surfactants in layered double hydroxides

Lumbidzani Moyo · Nontete Nhlapo · Walter W. Focke

Received: 27 June 2008 / Accepted: 6 August 2008 / Published online: 26 August 2008

Abstract Anionic surfactant intercalated layered double hydroxides (LDH) of high purity are easily prepared via direct coprecipitation and also by the ion exchange method provided that the precursor contains a monovalent anion, e.g., LDH–Cl or LDH–NO_3. However, LDH–CO_3 is an attractive starting material as it is commercially available in bulk form owing to large-scale applications as a PVC stabilizer and acid scavenger in polyolefins. Thus, intercalation of dodecyl sulfate and dodecylbenzenesulfonate into a commercial (LDH) with approximate composition $[Mg_{0.654}Al_{0.346}(OH)_2](CO_3)_{0.173} \cdot 0.5H_2O]$ was explored. Direct ion exchange is difficult as the carbonate is held tenaciously. In the regeneration method it is removed by thermal treatment and the surfactant form obtained by reaction with the layered double hydroxide that forms in aqueous medium. Unfortunately the resulting products are impure, poorly crystallized and only partial intercalation is achieved. Better results were obtained using water-soluble organic acids, e.g., acetic, butyric, or hexanoic acid, to aid decarbonation of LDH–CO_3. Intercalation proceeded at ambient temperatures with the precursor powder suspended in an aqueous dispersion of the anionic surfactant. The carboxylic acids are believed to assist intercalation by facilitating the elimination of the carbonate ions present in the anionic clay galleries.

Introduction

Layered double hydroxides

The Mg–Al layered double hydroxides (LDH) are anionic clays with the general formula $[Mg_{1-x}Al_x(OH)_2]^{x+}A^{y-}_{x/y} \cdot zH_2O$ where A is a charge balancing anion and x is the fractional aluminum substitution in the layers. It usually varies from 0.20 to 0.36 [1–6]. LDH are synthetic analogues of the natural mineral hydrotalcite $[Mg_6Al_2(OH)_{16}CO_3 \cdot 4H_2O]$. These materials feature a brucite-like $[Mg(OH)_2]$ stacked sheet structure in which the cations are octahedrally coordinated by six oxygen atoms as hydroxides. A net positive charge of the sheets arises from the partial replacement of Mg^{2+} with Al^{3+} ions. The interlayer contains water and charge balancing anions, e.g., carbonate ions in LDH–CO_3 [7]. The three dimensional structure of the clay is maintained by a combination of electrostatic forces and hydrogen bonding interactions between the layer and interlayer anions or molecules [6]. Hydrophobic interactions also play a role when the inserted anions contain long aliphatic chains [8–10]. The basal spacing of the (003) planes in brucite is 0.47 nm [11]. In LDH–CO_3 structures it increases slightly with a decrease in the fractional aluminum substitution. Bellotto et al. [12] give values of 0.76 and 0.79 nm for $x = 0.36$ and $x = 0.17$, respectively.

Surfactants and surfactant aggregates

Surface active agents (surfactants) are molecules with an amphiphilic nature [13]. Their chemical structure contains two parts with very different polarities: a polar hydrophilic head group (e.g., a sulfonate ion) and a non-polar hydrophobic tail. The latter is often represented by a linear alkane chain segment. The hydrophilic head group shows

---

L. Moyo · N. Nhlapo
Department of Chemistry, Institute of Applied Materials,
University of Pretoria, Lynnwood Road,
Pretoria 0002, South Africa

W. W. Focke (✉)
Department of Chemical Engineering, University of Pretoria,
Lynnwood Road, Pretoria 0002, South Africa
e-mail: walter.focke@up.ac.za

strong affinity for water but is not very compatible with non-polar solvents. The hydrophobic segment is soluble in non-polar solvents but has a low affinity for water and other polar solvents. Surfactants usually have a relatively low solubility in water and show a distinct preference to adsorb on available surfaces and interfaces. This leads to reduced surface and interfacial tensions, respectively.

Surfactant molecules self-organize into micellar aggregates above the critical micelle concentration or CMC. Just above the CMC the micelles usually have a spherical shape with surfactant molecules arranged such that the hydrophilic part is on the outside and the hydrophobic part in the center. As the concentration is increased, the micelles coalesce to first form elongated 'worm-like' tubes and later convert into lamellar sheets of organized molecules [14].

Surfactant adsorption on clay surfaces

Clay particles present two different surfaces for interaction with surfactants. It is usual to use the expression "adsorption" when the interaction is limited to aggregation of the surfactant on the outside surfaces of the clay particles. The phrase "intercalation" refers to situation where the surfactant molecules additionally aggregate inside the galleries, i.e., between pairs of adjacent clay sheets. Crepaldi et al. [15] gives a short overview of surfactant intercalation into LDH.

The adsorption of surfactants is a type of aggregate formation on the mineral surface. Harwell et al. [16] refer to these as admicelles to emphasize the micelle-like aspects of their structure and behavior. Bitting and Harwell [17] found that the degree of adsorption of dodecyl sulfate salts on oxide minerals is a function of pH, counterion type, and counterion concentration. Ionic surfactant aggregate formation is favored at higher counterion concentrations. There is also a tendency for monovalent counterions to adsorb between the surfactant aggregate and the mineral surface. The extent of adsorption process depends on the pH as well as the nature of the counterion type as it is determined by a combination of steric and surface complexation effects. The planar geometry of admicelles present is expected to provide for more favorable steric interactions compared to spherical micelles in the bulk solution.

Clay intercalation

Self-assembly is the process whereby small pre-existing subunits spontaneously organize themselves into an ordered state or structural arrangement. The formation of lamellar micelles by surfactants molecules in solution is a typical example [18]. Interactions that promote self-assembly include electrostatic attractions, hydrogen bonding, and hydrophobic interactions among others [19]. Intercalation is defined as a reversible insertion of mobile guest species into a crystalline host lattice during which the structural integrity of the latter is formally conserved [20].

Adsorption and intercalation of surfactants in LDH

Pavan et al. [21] concluded that adsorption on LDH mirrors the surfactant adsorption behavior on mineral oxides with respect to the effects of pH, counter ion type, and ionic strength [17]. Dèkány and Haraszti [22], and Pavan et al. [21, 23, 24] found that anionic surfactants such as sodium dodecyl sulfate (SDS) and sodium dodecylbenzenesulfonate (SDBS) adsorb on the LDH–CO_3 crystal surfaces rendering them hydrophobic. Pavan et al. [21] explicitly state that these surfactants do not intercalate when the LDH contains the difficult to exchange carbonate anion. This was confirmed by Ulibarri et al. [25] with respect to the interaction between dodecylbenzenesulfonate (SDBS) and Mg_3Al–LDH–CO_3 at ambient conditions. It seems that temperature plays an important role too. While at 25 °C SDS only absorbs on LDH–CO_3 [21] some intercalation was observed when the mixture was heated to 70 °C [26]. However, SDBS still did not intercalate at the latter temperature [26], but partial replacement of carbonate did occur under reflux conditions and very long reaction times [10]. Apparently the high affinity of the layered double hydroxide for the carbonate ion prevents the latter's displacement by the sulfonate ions even at high contact temperatures. Xu and Braterman [10] argue that the replacement of carbonate with RSO_3^- is kinetically rather than thermodynamically controlled as the carbonate is very tightly bonded [27, 28], and its removal requires the scaling of a high activation energy barrier.

Direct intercalation of LDH clays involves ion exchange. It is regarded as a form of spontaneous self assembly of the guest molecules or ions between the brucite-like layers of the crystal lattice [29]. Layered host lattices can adapt to the geometry of the inserted guest species by adjustment of the interlayer separation. Intercalation of organic compounds creates diverse types of supramolecular structures in the clay interlayer [30]. Linear molecules with appropriate functional groups self-assemble into monolayers or bilayers between the sheets of LDH [20]. The intercalation of surfactants such as SDS from aqueous solution can be viewed as a change in the nature of the micelle structure from spherical to lamellar [15]. The internal hydoxy sheet surfaces are similar to the surface planes presented to the outside. Thus, it is expected that intercalation behavior will mimic that of the adsorption process. For example, it is found that monovalent anions and water co-intercalate [8, 9, 31]. However, there are key differences. The intercalating guest molecule is now affected by, and must interact with, two parallel clay surfaces in its vicinity. This constraint enforces a greater degree of order within the galleries than is required at the free outside clay surfaces. Displacing multivalent resident ions may also be more difficult. They may neutralize charges on opposite sheets thereby making parting, to allow larger guests to move in, more difficult. In addition, carbonate ions also interact strongly with both surfaces via hydrogen bonding forces [32, 33].

Guest surfactant molecules usually assemble in either a monolayer or a bilayer format. The actual monolayer arrangement of surfactant chains in intercalated LDH corresponds to two interdigitated anti-parallel half-monolayers [10, 34]. Kopka et al. [3] derived equations for estimating the basal spacing of mono- and bilayer intercalated clays based on the following assumptions: (i) Alkyl chain substituents assume an extended chain conformation; (ii) the methylene bond length equals to 0.127 nm, and (iii) the slant angle is independent of the chain length.

$$\text{Monolayer:}\quad d_L = d_0 + d_1 + d_2 + 0.127n\cos\alpha \qquad (1)$$

$$\text{Bilayer:}\quad d_L = 2d_0 + 2d_1 + d_3 + 0.254n\cos\alpha \qquad (2)$$

Here, d_L is the basal spacing, n represents the number of carbon atoms in the aliphatic chain; α is the chain tilt angle to LDH layer plane; d_o measures the vertical dimension of the head group taking into account its relative intercalated orientation; d_1 and d_2 are the distances between the center plane of the brucite-like sheets and the terminal (ionized) head group and tail ends respectively; d_3 is the distance between the two facing terminal methyl groups in the bilayer structure. Note that both d_1 and d_2 can be affected by the presence adsorbed water, solvents molecules or other ions in the galleries.

The extended length of SDBS is about 2.26 nm [35]. Meyn et al. [36] suggest that intercalated dodecylbenzenesulfonate ions orient their extended alkyl chains into a perpendicular position with the benzene ring tilted toward the layer. This proposed arrangement was supported by You et al. [37]. Instead, Xu and Braterman [10] and Zhao and Nagy [38] contend that (i) the benzene rings are oriented perpendicularly to allow for three point attachment of the sulfonate group to the hydroxide layer, and (ii) that the alkyl chains are tilted at ca. 56° with respect to the layer planes in order to facilitate their close packing. They argue that such anti-parallel arrangement also reduces the electrostatic repulsion between the anion head groups and effectively maintains the hydrophobic interactions between the hydrocarbon chains. These two proposals can be tested by plotting the basal spacing against the chain carbon number (Fig. 1). According to Eqs. 1 and 2, the tilt angle can be calculated from knowledge of the type of intercalation and the slope of the d_L versus carbon number plot. Least square data fitting of the data shown in Fig. 1 yielded α values of 60.0°, 68.8°, and 61.8° for alkyl sulfonates in Mg_2Al–LDH [39]; alkyl sulfates in Zn_2Al–LDH [3], and alkylbenzene sulfonates in Mg_2Al–LDH [36], respectively. These values, while somewhat higher than the expected angle of 56°, do provide support for the Xu and Brateman's [10] proposal.

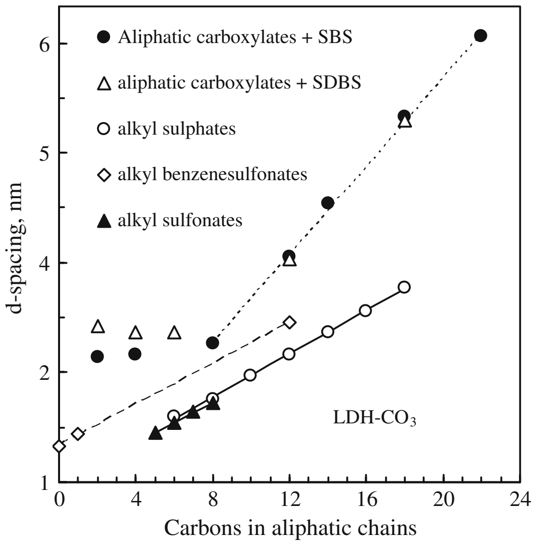

Fig. 1 Effect of alkyl chain length on the basal spacing: (▲) Alkyl sulfonates in Mg_2Al–LDH [39]; (○) alkyl sulfates in Zn_2Al–LDH [3]; (◇) alkylbenzene sulfonates in Mg_2Al–LDH [36]; LDH–"carboxylates" prepared in the presence of SDS (●) or SDBS(Δ) (this work and Nhlapo et al. [61])

The LDH–DS and LDH–DBS data collated in Table 1 show a considerable spread in the reported basal spacing values. Clearly the observed d-spacing of LDH–CO_3 and other intercalated derivatives depends on a number of factors. Much of the variation can be attributed to differences in the degree of hydration, i.e., the presence or absence of interlayer water [3, 36, 40, 41]. It also explains the variations induced by the drying procedure including the effect of temperature drying temperature: Meyn et al. [36] indicate that vacuum drying at 65 °C reduces the basal spacing of about 0.3 nm owing to removal of the adsorbed water from the interlayer. Interestingly, the aliphatic chain tilt angle is also affected by the presence of the interlayer water [41]. Zhao and Nagy [38] state that the intercalation pH influences the d-spacing of intercalates prepared by the coprecipitation method. For LDH–DS in particular it is claimed that the interlayer spacing is affected by the method of synthesis [41], the LDH Mg:Al ratio [38], and the intercalation pH [31, 38]. Clearfield et al. [31] found that, as the exchange pH was increased, so did the basal spacing although, surprisingly, the amount of SDS in the interlayer decreased. This communication will attempt to provide a rationalization for this unexpected and unexplained pH dependence.

Table 1 Effect of the intercalation method and Mg:Al ratio on the d-spacing of LDH–DS and LDH–DBS

Intercalation method	d-Spacing[a] (nm)		Reference
LDH Mg:Al ratio	LDH–DS	LDH–DBS	
Reconstitution			[54]
0.250		2.64	[50]
0.250		3.01	[25]
0.330	2.68	2.95	[57]
0.333	2.62	2.95	[56]
0.340	2.6		[21]
Coprecipitation			
0.171	4.03		[10]
0.205	3.66		
0.250	2.63		[42]
0.250		2.68	[70]
0.254	2.54		[38]
0.290	2.63		[92]
0.301	2.60		[38]
Ion exchange			
0.171	2.92		[38]
0.175		2.74	[50]
0.204		2.74	
0.205	2.78		[38]
0.250	2.27	2.66	[37]
0.250		2.95	[36]
0.254	2.43		[38]
0.256		2.66	[50]
0.301	2.58		[38]
0.323	2.09	Failed[b]	[26]
0.333	2.42	2.96	[49]
0.333	2.6		[93]
0.333		2.87	[50]
0.333		3.05	[10]

[a] Where applicable as prepared before drying

[b] Intercalation failed

LDH surfactants intercalation methods

Miyata and Kumura [7] first intercalated LDH with different organic anions. Newman and Jones [41] and Crepaldi et al. [15] give overviews of surfactant intercalation in LDH. Intercalated LDHs can be prepared by direct synthesis methods, e.g., hydrothermal crystallization of gels formed by the coprecipitation of the M^{2+} and M^{3+} hydroxides in the presence of the required organic anion [10, 15, 31, 38, 42, 43]. Hussein et al. [44] used microwave heating to accelerate the co-precipitation driven intercalation of SDS into Zn_4Al–LDH.

Indirect methods utilize suitable LDH precursors prepared by direct synthesis. Indirect intercalation involves the modification and treatment of the host and finally the insertion of the guest molecules inside the layer. Crepaldi et al. [45] identified three main indirect techniques: (i) direct anion exchange; (ii) LDH reconstruction from a layered double oxide form obtained by calcinations of a suitable precursor; and (iii) anion replacement by elimination of the precursor interlamellar species.

(i) *Direct anion exchange*: Direct ion exchange was pioneered by Miyata and Kumura [7]. First consider the exchange of simple anions, e.g., the replacement of nitrate ions in LDH–NO_3 with chloride ions from aqueous solution. The mass action relationship is written as:

$$\text{Scheme I:}\quad \mathrm{Cl^-_{(aq)}} + \{\mathrm{LDH}\}^+\mathrm{NO_3^-} \overset{K^{\mathrm{Cl}}_{\mathrm{NO_3}}}{\rightleftharpoons} \{\mathrm{LDH}\}^+\mathrm{Cl^-} + \mathrm{NO^-_{3(aq)}}$$

Here {LDH} represents a clay subunit commensurate with a single positive charge or Al atom. In this communication $\{\mathrm{LDH}\} = \{\mathrm{Mg_2Al(OH)_6}\}$ is used as archetype for discussion and illustration purposes. The selectivity coefficient $K^{\mathrm{Cl}}_{\mathrm{NO_3}}$, the intercalation of the chloride anion relative to chloride ion in the ion exchange reaction is defined as follows [34, 46]:

$$K^{\mathrm{Cl}}_{\mathrm{NO_3}} = \frac{X_{\mathrm{Cl}} S_{\mathrm{NO_3}}}{X_{\mathrm{NO_3}} S_{\mathrm{Cl}}}$$

X_{Cl} and $X_{\mathrm{NO_3}}$ represent the fraction of chloride and nitrate anions present in the clay when equilibrium has been reached. S_{Cl} and $S_{\mathrm{NO_3}}$ are the equivalent fractions of these ions present in the aqueous solution. The exchange may also involve heterovalent ions as in Scheme II:

$$\text{Scheme II:}\quad {}^1\!/_2\,\mathrm{CO^{2-}_{3(aq)}} + \{\mathrm{LDH}\}^+\mathrm{NO_3^-} \overset{K^{\mathrm{Cl}}_{\mathrm{NO_3}}}{\rightleftharpoons} \{\mathrm{LDH}\}^+[\mathrm{CO_3^{2-}}]_{0.5} + \mathrm{NO^-_{3(aq)}}$$

In this case the selectivity coefficient takes the form [46]:

$$K^{\mathrm{CO_3}}_{\mathrm{NO_3}} = \frac{S_{\mathrm{NO_3}}\sqrt{X_{\mathrm{CO_3}}}}{X_{\mathrm{NO_3}}\sqrt{S_{\mathrm{CO_3}}}}$$

Miyata [46] reports $\log_{10} K^{\mathrm{CO_3}}_{\mathrm{NO_3}} \approx 1.84$ and $\log_{10} K^{\mathrm{Cl}}_{\mathrm{NO_3}} \approx 0.26$ so that $\log_{10} K^{\mathrm{CO_3}}_{\mathrm{Cl}} \approx 1.58$.

Thus, direct intercalation of LDH-A is achieved by direct contact with a suitably concentrated aqueous or non-aqueous solution of the desired anionic surfactant [3, 10, 31, 36–38, 47–49]. Owing to the tenacity by which carbonate is held, it is customary to use anions such as chloride [37, 50] or nitrate [3, 36, 42, 47]. The intercalation reaction for a surfactant such as SDS into LDH–Cl as may be expressed as follows [34, 46]:

$$\text{Scheme III:}\quad \mathrm{R{-}OSO_3^-Na^+_{(aq)}} + \{\mathrm{LDH}\}^+\mathrm{Cl^-} \overset{K^{\mathrm{DS}}_{\mathrm{Cl}}}{\rightleftharpoons} \mathrm{R{-}OSO_3^-}\{\mathrm{LDH}\}^+ + \mathrm{Na^+_{(aq)}} + \mathrm{Cl^-_{(aq)}}$$

Kopka et al. [3] describe intercalation by anion exchange of Zn_2Cr–LDH–NO_3 with alkyl sulfate ions

$[C_nH_{2n+1}SO_4^-$ with $n = 6, 8, \ldots, 18]$ as well as dodecyl glycol ether sulfate ions $[C_{12}H_{25}(OCH_2CH_2)_nSO_4^-$ with $n = 0, 1, 2, 4]$. They claim that the exchange reaction proceeds to 90–95% of theory. Monolayer intercalation was observed. However, co-intercalation with alkanols and alkyl amines of similar chain lengths lead to the formation of bilayer structures. Water and small organic molecules, e.g., diols, NMF, DMSO, etc., co-intercalated as well. Meyn et al. [36] studied the intercalation of anionic surfactants by such anion exchange into a wide range of LDH compounds. They observed that dodecylbenzenesulfonate intercalated as monolayers while secondary alkyl sulfonates intercalated as bimolecular layers.

You et al. [37] investigated the intercalation of sodium octyl sulfate (SOS), SDS 4-octylbenzenesulfonate (SOBS) and SDBS into Mg_3Al–LDH–Cl via ion exchange in aqueous medium. They found that the equilibrium amount of surfactant intercalated decreased in the order SDS > SOBS > SDBS > SOS. SOS also formed bilayers but the others exhibited monolayer arrangements. Xu and Braterman [10] prepared Mg_2Al–LDH–DBS. The intercalated dodecylbenzenesulfonate product had a d-spacing of 3.05 nm consistent with anti-parallel monolayer packing of interpenetrating chains.

Crepaldi et al. [45] describe a variation of the ion exchange method based on the formation and organic phase extraction of a salt between dodecyl sulfate and a cationic surfactant.

Anbarasan et al. [26] attempted the direct ion exchange reaction using Mg_2Al–LDH–CO_3 at 70 °C. They found no evidence for the intercalation of SDBS. The XRD spectrum of the product obtained using SDS features new peaks at lower angles consistent with a basal spacing of 2.09 nm which Anbarasan et al. [26] interpret as providing evidence for some monolayer intercalation of SDS.

True ion exchange reactions are topotactic in nature implying that any layer stacking defects in the precursor will also appear in the pillared LDH product [51]. However, Xu and Braterman [10] observed changes in crystal habit on intercalating SDS in LDH at elevated temperatures. This implies that at least some recrystallization must have accompanied the intercalation process.

(ii) *The LDH reconstruction method*: Comprises a hydrothermal reconstitution of calcined LDH carbonates in the presence of the desired anion in carbonate-free water [15, 21, 37, 51–57]. As discussed above, carbonate anions do not readily ion exchange owing to strong electrostatic and hydrogen-bonding interactions. Calcining a suitable precursor, e.g., LDH–CO_3 at 400–500 °C produces a dehydroxylated and decarbonated layered double oxide (LDO) form. From this the original clay can be reconstructed, in an intercalated form, by treatment with an aqueous solution of the required anion. The mechanism is believed to entail the fast rehydration of the oxide with intercalation of OH^- anions, followed by a slow anion exchange of the latter with other anions [15]. The formation of the pure hydroxide (LDH–OH) form requires reconstruction in pure water and total exclusion of CO_2, e.g., a nitrogen atmosphere [51]. Chibwe and Jones [54] intercalated SDS, *p*-toluene sulfonate, and other ions using the reconstitution method. Chibwe and Jones [54], Dimotakis and Pinnavaia [51], and Hansen and Taylor [58] claim that intercalation of anionic surfactants and other anions into the LDH–OH form is facilitated by the presence of glycerol. You et al. [37] and Costa et al. [57] point out shortcomings of the reconstruction method. When applied to organic anions, mixed phases may be produced [54], and it is difficult to avoid formation of carbonate forms. Products often show a perforated surface morphology and feature broad XRD peaks indicative of poorly developed crystallinity. This communication will show that, for the intercalation of SDS, the reconstruction method holds additional drawbacks.

(iii) *Anion exchange by elimination of a precursor interlamellar species*: Carlino et al. [59, 60] and others [26, 61, 62] showed that thermal intercalation takes place when the LDH–CO_3 is brought into direct contact with pure molten organic acids. This method has, as far as we could ascertain, not yet been used to intercalate anionic surfactants of the sulfate or sulfonate type.

LDH applications

LDH-type anionic clays, as such or in their calcined form, have existing and many potential applications [63]. In medicine they are utilized as antacids and antipeptins. In polymer technology they function as halogen scavengers, flame retardants, and PVC stabilizers. They are employed as catalysts and catalyst supports and their absorbent and ion exchange properties are of interest in waste water treatment. Surfactant intercalated layered double hydroxides are of interest for a variety of reasons [41]. Hydrophobization of the LDH by ion exchange yields new types of thickening agents. It also facilitates sorption of nonionic organic compounds [30], e.g., trichloroethylene and tetrachloroethylene [50]. The distinctive properties of these modified layered double hydroxides permit a wide range of uses including polymer additives [64], precursors for catalysts [63, 65], and magnetic materials [64]. Nanocomposites can be prepared by exfoliation within polymer matrices [57, 65–69]. Their generally non-toxic nature and membrane-like structure can be harnessed to protect, carry, deliver, and controllably release active compounds such as pesticides [70], pharmaceuticals and even genes [65, 71]. They can be used as adsorbents to remove contaminants from water [38, 56].

Due to the wide-ranging utility of LDH intercalates, it is of interest to consider environmentally friendly and energy efficient methods of intercalation that yield products of an acceptable quality. LDH–CO_3 is currently available as a bulk raw material owing to growing PVC stabilizer applications. Our interest is in upgrading this basic starting material by suitable intercalation procedures. Previously we reported on the surfactant-mediated intercalation of long chain fatty acids into LDH–CO_3 [61]. The method is a refinement of the Carlino et al. [59, 60, 72] melt intercalation method with anion exchange facilitated by elimination of the carbonate species. This communication reports on a similar approach based on contacting aqueous suspensions of LDH–CO_3 with combinations of a short chain aliphatic carboxylic acid and an anionic surfactant, e.g., SDS or sodium dodecylbenzene sulfate (SDBS). It was found that this simple procedure, conducted at ambient conditions without exclusion of CO_2, provides a facile one-pot method for intercalating these surfactants in LDH.

Experimental

Materials

LDH–CO_3 (Hydrotalcite Grade HT 325) was supplied by Chamotte Holdings. It contained silica and magnesium carbonate as minor impurities. Distilled water was used in all experiments. High purity (>98%) SDS and SDBS were purchased from Fluka–Biochemika. Croda chemicals supplied the octanoic and dodecanoic acids. Myristic acid was obtained from BDH Chemicals. Butanoic acid (>99%) was supplied by Merck. AR grade glacial acetic acid and acetone (99.5%) were supplied by Saarchem UnivAR. Aqueous ammonium hydroxide solution (25%) was procured from Promark chemicals. Potassium bromide (Uvasol KBr, Merck) was used for preparing samples for FTIR spectra recording.

Sample preparation

Surfactant intercalation experiments were carried out using variations of the following representative procedure: 75 g SDS (0.26 mol) and 15 g acetic acid (0.25 mol) were dispersed in 1.5 L distilled water and the pH adjusted to $pH = 10$. To this 20 g HT-325 (LDH–CO_3 approximating $[Mg_{0.66}Al_{0.34}(OH)_2](CO_3)_{0.17} \cdot \frac{1}{2}H_2O$ (ca. 0.10 mol Al) was added slowly while stirring. The emulsion–suspension was left to stir overnight. The pH was again adjusted to $pH = 10$ each morning by adding dilute ammonia or NaOH solution if required. It was noted that pH dropped to as low as $pH = 7.2$ overnight. The mixture was allowed to react at ambient temperature for a total of 2 days. The product was recovered by centrifugation, washed four times with distilled water, and once with acetone. After each washing the solids were separated from the liquid by centrifugation. The product was allowed to dry at room temperature. This experiment was repeated leaving out the acetic acid or the SDS. The effect of raising the reaction temperature to 65 °C or 80 °C as well as using reduced amounts of the SDS and/or the acetic acid was also investigated. Similar experiments were done using sodium dodecyl sulfate (SDBS) in place of the SDS or magnesium hydroxide in place of LDH–CO_3. Fatty acid intercalation experiments followed procedures similar to the preparation of LDH–laurate: 20 g LDH–CO_3 (0.10 mol Al), 40 g SDS (0.26 mol), 76.9 g lauric acid (0.38 mol), and 20 g HT-325 were dispersed in 1 L distilled water at 70 °C and allowed to stir continuously for 3 days. Lauric acid was divided into three equal portions. One part was added at the start of the experiment and the two other portions added every subsequent day. When required, dilute NH_4OH was added to the mixture in order to maintain the pH at $pH = 10 \pm 0.5$.

Additional LDH–DS and LDH–DBS samples were prepared by the regeneration method described by Costa et al. [57]. In this case LDH–CO_3 was first calcined at 450 °C for 3 h and then stirred in a suspension of the relevant surfactant. These samples were analyzed by TG and XRF to determine organic and the sodium contents, respectively. Samples prepared using LDH with $x \approx 0.33$ were donated by Dr Costa and analyzed as such.

A mixture of LDH–stearate and magnesium stearate was prepared as follows: LDH was intercalated with stearate using the standard procedure described above by reacting 20 g HT 325 with 40 g stearic acid in the presence of 54.4 g SDS at 80 °C. After completion of the reaction, 56.54 g Mg stearate was added over a period of a further 2 days. Thereafter the mixture was allowed to stir for another 4 days at 80 °C.

Characterization

The particle size distribution and BET surface area of the precursor LDH were determined using a Malvern Mastersizer Hydro 2000MY instrument and a Micromeritics Flowsorb II 2300 instrument, respectively.

Elemental composition was determined by XRF analysis. The intercalated materials were ashed before analysis in order to reduce their bulk. These samples were ground to <75 μm in a tungsten carbide mill and roasted at 1,000 °C. Then, 1 g sample was added to 9 g $Li_2B_4O_7$ and fused into a glassed bead. Major element analysis was executed on the fused bead using an ARL9400XP + spectrometer.

Powder samples were viewed on a JEOL 840 SEM scanning electron microscope under low magnification. They were prepared as follows: A small quantity of the powder products or the LDH–CO_3 precursor was placed onto carbon tape on a metal sample holder. Excess powder was removed using a single compressed air blast. The samples were then coated five times with gold under argon gas using the SEM autocoating unit E5200 (Polaron equipment LTD).

Thermogravimetric analysis was conducted on a Mettler Toledo A851 TGA/SDTA machine. Powder samples of ca. 10 mg were placed in 70 μL alumina open pans. Temperature was scanned at 10 °C/min in air range from 25 to 800 °C.

FTIR spectra were recorded on a Bruker Opus Spectrophotometer. Samples were finely ground and combined with spectroscopic grade KBr in a ratio of 1:50, i.e., approximately 2 mg of sample and 100 mg of KBr. The mixture was pressed into a 13 mm φ pellet. The reported spectra were obtained over the range 400–4,000 cm^{-1} and represent the average of 32 scans at a resolution of 2 cm^{-1}.

XRD

Phase identification was carried out by XRD analysis on a PANalytical X-pert Pro powder diffractometer. The instrument features variable divergence and receiving slits and an X'celerator detector using Fe filtered Co K-α radiation (0.17901 nm). The X'Pert High Score Plus software was used for data manipulation.

Py/GC/MS

Small samples (3–4 mg) were analyzed on an Agilent GC/MS system fitted with a DB-17MS intermediate polarity GC column (30 m × 0.25 mm ID), an Agilent MSD 5971 mass spectrometer, and a CDS Instruments Pyroprobe 2000 pyrolyzer. Helium was used as carrier gas (1 mL/min; split 1:20).

Results

Table 2 lists sample designations and the thermal properties of the major compounds used or synthesized in this study. Table 3 presents XRF composition data as atom ratios relative to aluminum. The identification of the compound natures, as implied by the designations, is justified by the results presented below. Unless otherwise

Table 2 Sample designations, XRD determined basal spacings, and thermogravimetric data

Intercalated compound (carboxylic acid)	Method[a]	d_L (nm)	TG residual mass (%)			Clay (%)	Organic (%)
			150 °C	700 °C	800 °C		
Inorganic precursors							
LDH–CO_3 (HT 325)		0.763	98.09	59.15	58.82	100	–
LDH–CO_3 (Costa)		0.759	99.03	56.16	55.77	100	–
SDS experiments							
LDH + SDS (no acid)	e	0.760	98.41	58.68	–	98.9	1.1
LDH–DS (Costa)	r	2.69	94.09	65.03	64.70	na	na
LDH–DS (this study)	r	2.69	92.92	55.26	55.01	98.7	1.3
LDH–DS (acetic acid)	e	2.60	93.52	41.71	41.37	73.8	26.2
LDH–DS (butyric acid)	e	2.59	92.52	33.33	33.02	59.5	40.5
LDH–octanoate	e	2.72	91.92	23.62	–	42.6	57.4
LDH–laurate	e	3.66	90.67	14.71	–	26.9	73.1
LDH–myristate	e	4.25	93.72	25.93		45.9	54.1
LDH–stearate	e	4.94	92.37	16.09	15.89	28.7	71.3
LDH–behenate	e	6.07	95.7	9.00		15.6	84.4
SDBS experiments							
LDH–DBS (Costa)	r	3.07	91.57	41.06	40.85	74.4	25.6
LDH–DBS (this study)	r	3.04	92.41	45.77	45.50	81.5	18.5
LDH–DBS (acetic acid)	e	2.88	93.55	37.99	36.92	65.8	34.2
LDH–DBS (butyric acid)	e	2.84	92.52	33.33	33.02	59.5	40.5
LDH–DBS (hexanoic acid)	e	2.84	92.99	38.68	38.24	68.6	31.4
LDH–DBS (lauric acid)	e	3.64	91.69	18.56	18.30	33.0	67.0
LDH–(DBS + dodecyl alcohol)	e	3.15	93.64	36.17	35.84	63.1	36.9

[a] e = acid assisted decarbonation method; r = regeneration method

Table 3 XRF results with composition expressed as atom ratios relative to aluminum

Intercalation	Method		Mediated ion exchange		Regeneration	
Atom	LDH	LDH–laurate	LDH–DS	LDH–DBS	LDH–DS	LDH–DBS
Mg	1.89	2.31	1.87	2.16	2.27	2.13
S	0.024	0.027	0.356	0.266	0.467	0.127
Na	0.005	0.018	0.007	0.000	0.041	0.039
Si	0.051	0.050	0.041	0.047	0.049	0.062
Ca	0.002	0.021	0.002	0.004	0.018	0.018
Ni	0.003	0.002	0.002	0.004	0.004	0.004
Fe	0.003	0.004	0.003	0.003	0.004	0.003
x	0.346	0.278	0.349	0.317	0.304	0.318

indicated, all LDH–surfactant sample names refer to products prepared using acetic acid as intercalation aid and all LDH–carboxylates refer to samples prepared from the corresponding acid using SDS as mediating surfactant.

The Malvern particle size analysis of the LDH–CO_3 precursor revealed a bimodal particle size distribution with $d(0.1) = 1.0$ µm, $d(0.5) = 3.5$ µm, and $d(0.99) = 260$ µm. The measured BET surface areas were 7.9, 21.6, 17.0, 15.7, and 5.3 m^2/g for the $Mg(OH)_2$, LDH–CO_3, LDH–DS, LDH–DBS, and LDH–laurate, respectively. Table 3 reports the chemical composition of the precursor LDH and the intercalated products as determined by XRF analysis. The results are presented as atom ratios relative to the aluminum present. The data for the precursor indicate a value for $x = 0.346$ in the chemical formula $[Mg_{1-x}Al_x(OH)_2](CO_3)_{x/2} \cdot nH_2O$. XRF analysis points to values for x of 0.302, 0.349, and 0.317 for LDH–laurate, LDH–DS, and LDH–DBS, respectively.

Figure 2 shows SEM micrographs of the LDH–CO_3 precursor and selected intercalates. The LDH–CO_3 features the typical sand rose structure formed by numerous intergrown small crystallites [73]. The surfactant modified powders also show agglomerated platelets that are similar in size to those seen in the precursor. The LDH–laurate platelets differ in that they feature significantly larger lateral dimensions. Intercalates obtained by the regeneration method have an unusual perforated surface morphology.

Nhlapo et al. [61] described surfactant-assisted intercalation of fatty acids in the readily available LDH–carbonate. The carboxylic acids displace the basic carbonate anions and intercalate in bilayer form. Nhlapo's [61] method is, in essence, a refinement and improvement of the Carlino [59, 60] melt intercalation procedure. The intercalation reactions are conducted at temperatures just above the melting point of the acid concerned, with the LDH powder suspended in the acid oil-in-water emulsion. Surfactants, e.g., SDS, facilitate the intercalation process by emulsifying the molten acid and dispersing the LDH particles. This convenient and environmentally friendly method for carboxylic acids has several attractive features: Water is used as medium rather than organic solvents, clay calcinations are not necessary, and there is no need for working under a CO_2-free atmosphere.

It is well-established commercial practice to react magnesium hydroxide with molten stearic acid to produce magnesium stearate. In addition, LDH–CO_3 appears capable of intercalating variable amounts of stearate. This can exceed the anion exchange capacity by multiple factors [8, 9, 61]. Even so these products always contain some unreacted LDH–CO_3 as an impurity phase. These observations raise the question as to whether the Carlino melt method [59, 60] and Nhlapo's [61] procedure in fact deliver an intercalated product or just simply mixtures of magnesium and aluminum stearates together with unreacted LDH–CO_3. Figure 3 provides a possible answer to this question. It shows powder XRD spectra for recrystallized magnesium stearate, LDH–stearate (prepared in the presence of SDS), and a combination that contains approximately equal amounts of these two products. In the preparation of the latter mixture, the two compounds were heated together for an extended period of time in a water suspension containing SDS. The XRD spectra of the first two samples appear very similar. However, the spectrum for the mixture shows clear twinning of the basal reflections. This positively demonstrates the presence of two different phases and supports the assumption that the interaction of molten stearic acid with LDH yields the intercalated product instead of the metal soaps.

Figure 1 provides evidence that intercalation favors incorporation of long chain carboxylic acids above the anionic surfactants SDS and SDBS. The observed basal spacings (d_L) for the products obtained with either surfactant (SDS or SBS) are the same provided the aliphatic acid chain is sufficiently long. The dependence of d_L on the number of carbons in the carboxylic acid (n) was determined by a least square curve fit to the SDS data and yielded:

$$d_L = 0.810 + 0.241n \tag{3}$$

The magnitude of the observed basal spacing values implies bilayer intercalation. The slope $\Delta d_L/\Delta n = 0.241$ is

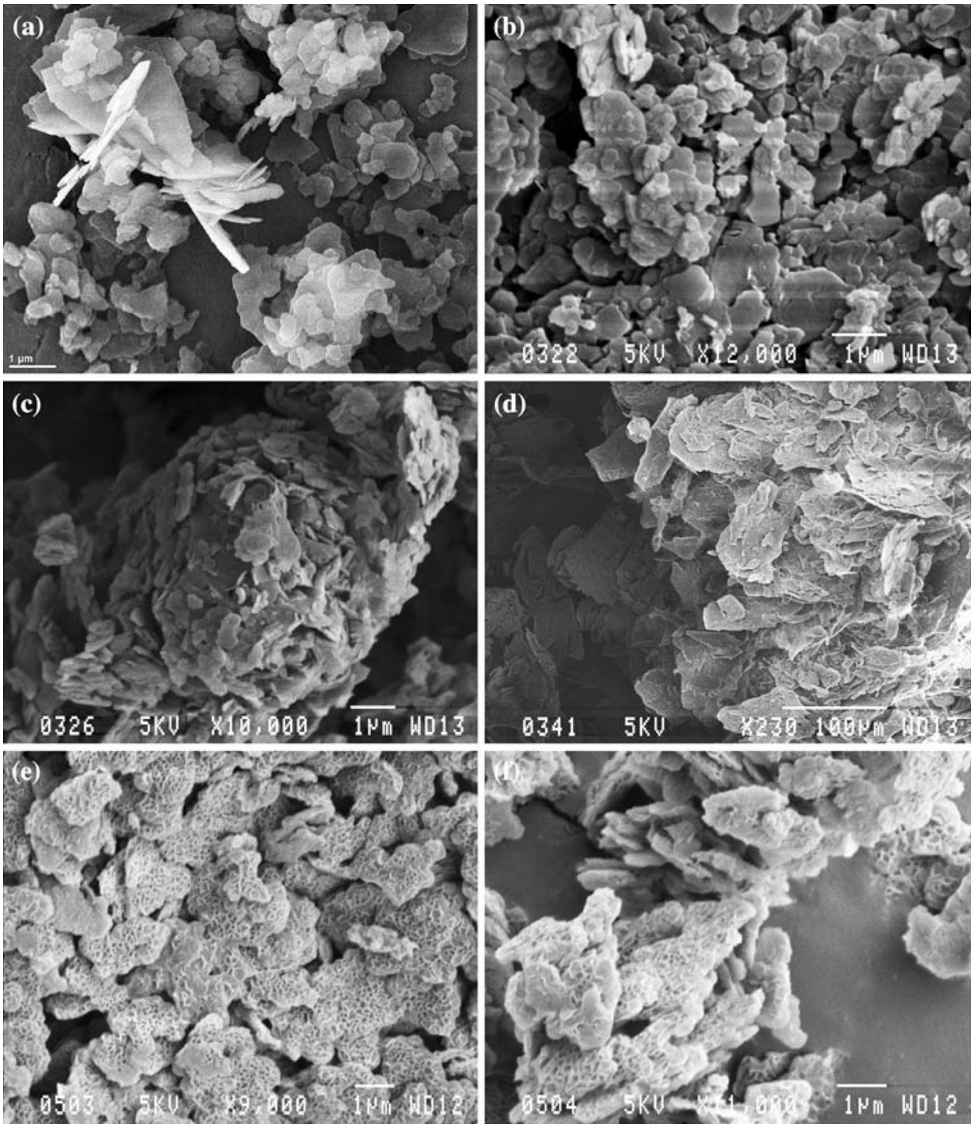

Fig. 2 SEM micrographs of (**a**) the LDH–CO_3 precursor; the products prepared by acetic acid aided intercalation (**b**) LDH–DS, (**c**) LDH–DBS, (**d**) LDH–laurate; and products obtained by the regeneration method: (**e**) LDH–DS and (**f**) LDH–DBS

consistent with a chain tilt angle of ca. 71.6° to the plane of the clay sheets [61].

Anbarasan et al. [26] previously found that SDBS on its own does not intercalate in LDH in aqueous suspension even when the reaction temperature is raised to 70 °C. However, they claim that some intercalation of SDS occurs under similar conditions but the basal spacing of the product was anomalously low ($d_L = 2.09$ nm cf. 2.67 nm). In the present study, intercalation of neat SDS and SDBS, as well as acetic acid on its own, was attempted under ambient conditions and pH = 10. The experimental basal spacing and TG data obtained for these products are presented in Table 2. They are in substantial agreement with the values determined for the precursor compounds, and thus indicate that no discernable intercalation occurred. However, the results were markedly different when the LDH was suspended in aqueous medium in the presence of mixtures of one of the surfactants together with a lower acid. Figure 1 shows that the basal spacing of the products obtained with acetic, butyric, or hexanoic acid, deviate considerably from the straight line dependence predicted by Eq. 3. For SDBS as surfactant, the corresponding *d*-values agree with each other to within experimental error ($d_L \approx 2.86$ nm). For SDS as surfactant, $d_L \approx 2.58$ nm for acetic and butyric acids. The experimental d_L values are in reasonable agreement with basal spacing values reported for LDH–DS and LDH–DBS as prepared by other methods (See Table 1). This implies that the presence of lower aliphatic acids facilitates intercalation of SDBS and SDS in LDH–CO_3 under mild conditions (ambient temperature and aqueous medium at pH < 10).

Figure 4 compares the X-ray diffractograms recorded for LDH–DS, LDH–DBS (both prepared in the presence of acetic acid), and LDH–laurate, with that for LDH–CO_3.

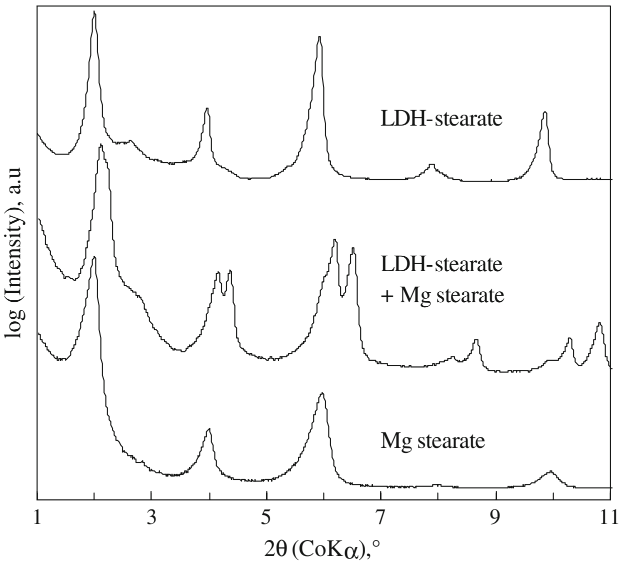

Fig. 3 Powder XRD spectra for recrystallized magnesium stearate, LDH–stearate, and a mixture of the two compounds. The LDH–stearate contains minor amounts of stearic acid as an impurity

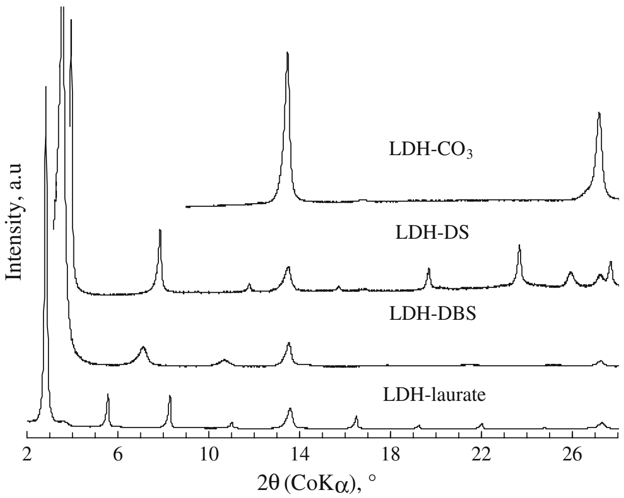

Fig. 4 X-ray diffractograms for LDH–CO$_3$, LDH–DS, LDH–DBS, and LDH–laurate obtained by the acetic acid mediated carbonate elimination method

The reflections at 0.76 nm ($2\theta = 13.2^{\circ}$) and 0.38 nm ($2\theta = 27.2^{\circ}$) are characteristic of LDH–CO$_3$. They are also present in the LDH–surfactant compounds indicating that they contain LDH–CO$_3$ as an impurity.

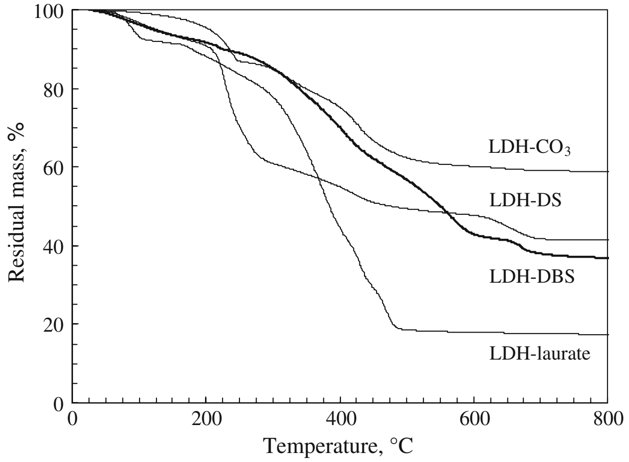

Fig. 5 Thermogravimetric (TG) mass loss curves for LDH–CO$_3$, LDH–DS, LDH–DBS, and LDH–laurate (prepared by the acetic acid mediated carbonate elimination method) obtained at a scan rate of 10 °C/min in an air atmosphere

Figure 5 shows the thermogravimetric traces for the LDH–CO$_3$ and some intercalates. The thermal decomposition of LDH–CO$_3$ occurs in three steps corresponding to loss of adsorbed and interlayer water, dehydroxylation, and a combination dehydroxylation–decarbonation reaction, respectively [52, 74, 75]. Thermal degradation of the intercalated layered double hydroxides takes place in several steps too. The first step is attributed to loss of interlayer water and is assumed complete at a temperature of 150 °C [59, 64, 76, 77]. Mass loss is effectively complete at 700 °C. The final residues may, to a first approximation, be assumed to have the same composition as the ash of the precursor provided sodium ions did not co-intercalate. This assumption allows one to make a rough estimate of the organic content of the initial sample and these are reported in Table 2.

All samples show gradual and progressive mass loss as the temperature is raised above 50 °C. Mass loss rates accelerate above 170, 210, 250, and 270 °C for LDH–laurate, LDH–DS, LDH–CO$_3$, and LDH–DBS, respectively. Below 550 °C the mass loss of LDH–DS exceeds that of LDH–DBS. The point where the mass loss rate accelerates cannot be regarded as a threshold limit for the stability of the LDH. Pyrolysis GC/MS of LDH–SDBS performed at 200 °C already reveals the liberation of a range of branched alkyl benzene compounds, i.e., typical SDBS degradation products. Application of this technique also confirmed that the SDBS did not co-intercalate with stearic acid. No aryl derivatives were found in the pyrolysis products of LDH–stearate obtained at 245 and 350 °C. Only aliphatic compounds were detected with the two major compounds identified as similar to C16 and C18 methyl esters.

The degree of aluminum substitution of the clay, characterized by the value that x assumes in the formula $[\mathrm{Mg}_{1-x}\mathrm{Al}_x(\mathrm{OH})_2](\mathrm{CO}_3)_{x/2} \cdot z\mathrm{H}_2\mathrm{O}$, also indicates the anion exchange capacity of the material. If intercalation had proceeded to completion, the expected residue levels on a dry, i.e., dehydrated clay basis are 63.4, 29.0, 26.9, and 34.3% for LDH–CO$_3$, LDH–DS, LDH–DBS, and LDH–laurate, respectively. This may be compared against the experimentally determined values of 60.0, 44.1, 39.1, and

18.9. The degree of intercalation was estimated using the values for x from the Al/Mg ratios indicated by XRF analysis (See Table 3) together with the residue levels determined by TG (See Table 2). The calculated values are 0.37, 0.46, and 2.51 for LDH–DS, LDH–DBS, and LDH–laurate. Thus, the extent of laurate intercalation exceeded the anionic exchange capacity of the clay by ca. 2.5 times. This high value is attributed to concomitant intercalation of non-ionized lauric acid and/or sodium laurate to provide for tight packing of the alkyl chains inside the clay galleries [8, 9, 61]. The sulfur to aluminum atom ratio should also provide an indication of the degree of intercalation of the anionic surfactants. Indeed, the S/Al value for LDH–DS is in good agreement with the degree of intercalation estimated from TG data. However, the S/Al = 0.266 value determined via XRF analysis for LDH–DBS is significantly lower than expected. It is possible that some sulfur may have been lost during the de-bulking heat treatment of the samples.

Figure 6 compares the FT-IR spectra of the unmodified layered double hydroxide (LDH–CO_3) with the LDH–surfactant intercalates. Costa et al. [57] provide a comprehensive analysis of the infrared absorption bands relevant to the present compounds. Therefore, the present discussion is limited to a short overview. The characteristic 446 cm^{-1} M–O lattice vibration band is present in all the samples. This is consistent with an intact LDH sheet structure. A broad band in the region 3,200–3,700 cm^{-1} is observed in all the compounds. It is attributed to OH stretching vibrations of the octahedral layer and intercalated water molecules [32, 78]. The shoulder at 3,063 cm^{-1} indicates hydrogen bonding of H_2O to CO_3^{2-} ion in the interlayer space [79–81]. As expected, the carbonate peak located at 1,367 cm^{-1} is well developed in LDH–CO_3. Its presence in the LDH–laurate indicates the unreacted LDH–CO_3 as an impurity. The triplet peaks observed in the range 2,850–2,965 cm^{-1} are due to C–H stretching. They confirm the presence of the alkyl chains of the surfactant anions in the intercalated LDH derivatives [31, 56, 57, 82]. Generally organic sulfate and sulfonate groups exhibit frequencies at 1,200–1,180 cm^{-1} [15, 31] and 1,420–1,370 cm^{-1} [26, 56, 70]. The former band is conspicuously absent in the LDH–laurate spectrum. This indicates that the LDH preferentially intercalated the laurate and that DS was not co-intercalated. The presence of a small peak at this position in the LDH–octanoate spectrum indicates that some DS did co-intercalate.

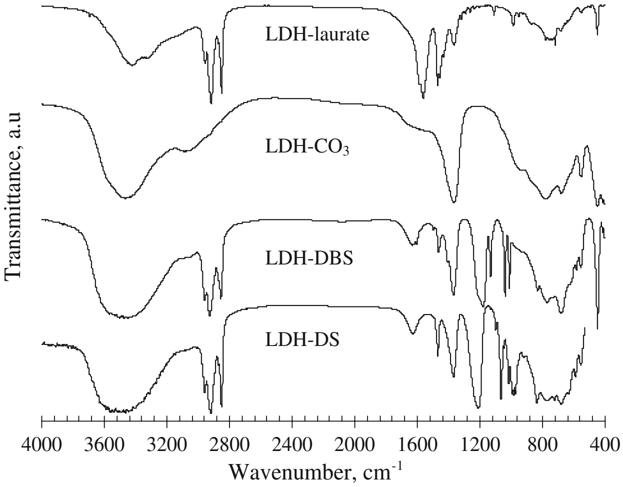

Fig. 6 FT-IR spectra for LDH–CO_3, LDH–DS, LDH–DBS, and LDH–laurate prepared by the acetic acid mediated carbonate elimination method

You et al. [37] used anion exchange to intercalate SDS and SDBS in LDH–Cl. They obtained AEC levels of ca. 72% using this method even though the solutions were sparged with nitrogen. Incomplete intercalation of LDH–DS was previously observed by Zhao and Nagy [38] using ion exchange and coprecipitation and by Costa et al. [57] for samples prepared using both anionic surfactants according to the regeneration method. In fact their data (surprisingly) show for their purported LDH–DS, a TG residue value that is higher than that found for the precursor LDH–CO_3. This indicates that the product obtained could not have been a pure LDH–DS. We therefore repeated these intercalation-by-regeneration experiments and reanalyzed samples supplied by Dr Costa. The TG and XRD results obtained for these samples are presented in Tables 2 and 3 and compared to the samples prepared using acetic acid as intercalation aid in Fig. 7. The products obtained using the current elimination methods are characterized by sharper and more intense XRD peaks than the regeneration-based samples. This suggests improved ordering and a better developed crystalline structure.

Consider the LDH–DS obtained by the regeneration method. The dominant series of broad peaks centered at 3.82°, 7.81°, and 8.00° (2.64 nm) in Fig. 7 are characteristic for monolayer intercalated SDS. The 0.74 nm basal spacing indicated by the peak at 14.0° is attributable to unreacted LDH–CO_3. Careful examination of the XRD spectrum for the regeneration-based LDH–DS reveals two additional series of XRD peaks. The large basal spacing (3.83 nm) indicated by the low-intensity, but sharp series of peaks at 2.70°, 5.34°, and 8.00° point to bilayer intercalation. This we attribute to co-intercalation of dodecanol with the dodecyl sulfate. This assumption is able to explain several anomalies in our experimental data for LDH–DS prepared by the regeneration method as well as observations by other investigators [26, 31, 37, 38, 57]. Firstly, while our LDH–DS has a high sulfur content (atom ratio S/Al = 0.467), the TG residue at 800 °C data indicates a very low organic content (See Table 2). Thus, there is insufficient dodecyl sulfate present to account for the high

Fig. 7 Comparing the X-ray diffractograms for LDH–DBS and LDH–DS prepared by reconstitution and the ion exchange by elimination method

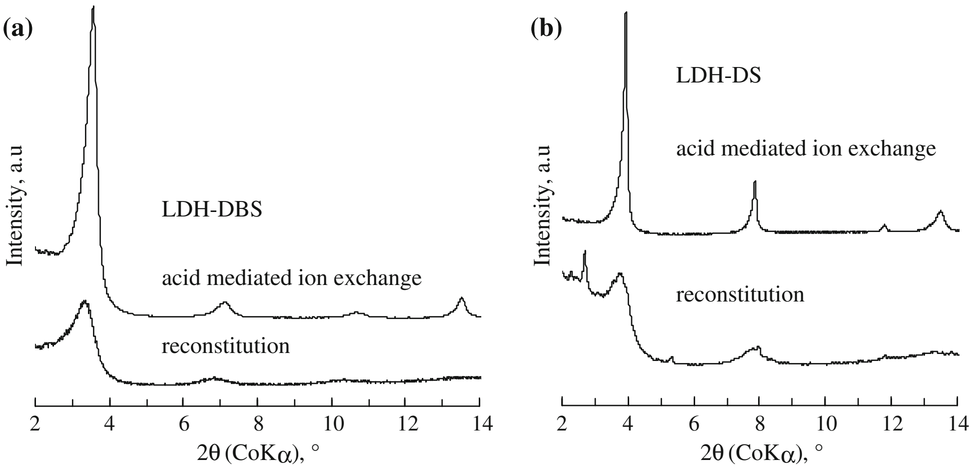

concentration sulfur in the sample. Since magnesium sulfate and aluminum sulfate are soluble, it is likely that the excess sulfur must be accounted for by the formation of LDH–SO_4. Indeed, the peaks at 11.8° and 23.9° (basal spacing 0.87 nm) are consistent with the presence of this phase as an impurity [52]. Kopka et al. [3] found that the alkanols co-intercalate with alkyl sulfates into Zn_2Cr–LDH forming a bilayer arrangement. They observed basal spacing of 4.15 nm for the combination of SDS and dodecanol in this LDH matrix. Thus, the present value for Mg_2Al–LDH is at least in the right ball park.

What could be the origin of the dodecanol and excess of sulfate ions? It is well known that sodium dodecyl sulfate hydrolyses at low pH [83, 84]. However, Angarska et al. [85] report that hydrolysis also occurs under highly basic conditions. Such hydrolysis would yield both the required sulfate ions and the dodecanol according to the following reaction:

$$\text{Scheme IV: } CH_3(CH_2)_{11}OSO_3^- + OH^- \rightarrow CH_3(CH_2)_{11}OH + SO_4^{2-}$$

Clearfield et al. [31] studied the effect of pH on the intercalation of SDS in Ni_4Al–LDH–Cl. It appears that they conducted their reactions at ambient conditions but reaction time was varied from 4 to 24 h. They found that, as the pH was increased, so did the interlayer spacing. However, surprisingly, the amount of dodecyl sulfate that was intercalated decreased. Our suggestion provides a rationalization of the pH effect observed by Clearfield et al. [31]. Hydrolysis of the surfactant releases sulfate ions that are preferentially intercalated. This reduces the ability of the clay to absorb SDS. The co-intercalation of the resultant dodecanol with the dodecyl sulfate explains the dramatic increase in the basal spacing. Interestingly, at pH = 9 and pH = 10, they observed basal spacing values of 36.6 and 42 nm, respectively. The latter value is just slightly larger than that found by Kopka et al. [3] for the co-intercalation of dodecanol and dodecyl sulfate. Zhao and Nagy [38] made similar observations with respect to a pH effect in Mg_4Al–LDH–DS and Mg_5Al–LDH–DS prepared by co-precipitation. When prepared at pH = 10, basal spacing values of 36.6 and 40.3 nm were found for these two compounds, respectively. Zhao and Nagy [38] used SDS in stoichiometric excess (1.5 times) and long reaction times at elevated temperatures (3 days at 65 °C). The degree of ion exchange was estimated from total organic content. They observed a decrease in the apparent degree of ion exchange with increase in the reaction pH. Again, we surmise that the high basal spacing is caused by the partial hydrolysis of the SDS and the subsequent co-intercalation of dodecanol with SDS. If this is indeed the case, the actual degree of ion exchange would be even lower and attributable to concomitant sulfate intercalation. Similar arguments may be relevant to explain the low degree of intercalation, as well as the reported bilayer nature of SOS intercalation, reported by You et al. [37].

Co-intercalation of the sodium salts was found to accompany that of the surfactant anions when the anion exchange or the direct precipitation methods are used to prepare LDH–DS [10, 31] or LDH–DBS [10]. However, the amounts tend to be small, e.g., Na/Al < 0.065 [10]. Table 3 indicates that even lower amounts of sodium were found in the present samples prepared using acetic acid as mediating agent. Quite the opposite holds for the sodium content of the samples prepared by the regeneration method. Considering Scheme I, this is not entirely surprising. Rehydration of the calcined clay (LDO) oxide initially results in rapid formation LDH–OH [86] according to Scheme V. Some magnesium (and aluminum) hydroxide will also dissolve. Both scenarios introduce excess hydroxyl anions and the pH of the water phase increases. We found that the hydration of the present LDO caused an initial rapid increase to pH = 10.7 with a slower rise to pH = 12 over a 24-h period. By comparison, when the same amount of LDH–CO_3 was suspended in distilled water, pH = 9.8 decreased to pH = 9.2 after 24 h.

Scheme V: $\text{LDO} + 3.5\text{H}_2\text{O} \rightarrow \{\text{LDH}\}^+\text{OH}^-$

Next these OH^- anions may be exchanged with other anions that are present in the mixture, e.g., intercalation of dodecyl sulfate ion according to Scheme VI:

$$\text{Scheme VI: } \text{R}{-}\text{OSO}_3^-\text{Na}^+_{(\text{aq})} + \{\text{LDH}\}^+\text{OH}^- \overset{K_i}{\rightleftharpoons} \text{R}{-}\text{OSO}_3^-\{\text{LDH}\}^+ + \text{Na}^+_{(\text{aq})} + \text{OH}^-_{(\text{aq})}$$

Parker et al. [87] measured the amount of anion that was absorbed by freshly calcined LDH after 24 h. They have found that the relative preference for anions follows the sequence:

$$\text{Sequence A: } \text{SO}_4^{2-} > \text{F}^- > \text{HPO}_4^{2-} > \text{Cl}^- > \text{B(OH)}_4^- > \text{NO}_3^-.$$

This matches the order of preferred affinity of anions in LDH (with $x \approx 0.3$) reported by Miyata [46]:

$$\text{Sequence B: } \text{CO}_3^{2-} \gg \text{SO}_4^{2-} \gg \text{OH}^- > \text{F}^- > \text{Br}^- > \text{Cl}^- > \text{NO}_3^- > \text{I}^-$$

Note that Bontchev et al. [88], instead, found that $\text{Br}^- > \text{Cl}^-$ for an LDH with $x \approx 0.25$. This suggests that the exact order of anion preference may depend to some extent on the Mg/Al ratio. In either case it is clear that LDH has a high affinity for the divalent sulfate ions and that they will easily replace hydroxyl ions present in the clay.

The mechanism of acid mediated decarbonation and intercalation

Bish [89] previously reported that the carbonate in LDH–CO_3 is readily exchanged with Cl^-, $\text{NO}_3{}^-$, and $\text{SO}_4{}^{2-}$ by treatment with dilute aqueous solutions of the corresponding inorganic acids. Iyi et al. [90, 91] proposed a credible two-step process to explain the decarbonation of LDH–CO_3 in the presence of dilute acid or acid–sodium salt mixtures. The first step is protonation of the carbonate and its conversion to the hydrocarbonate. Simultaneously another anion is incorporated into the interlayer space to maintain overall charge neutrality. Next the hydrocarbonate ion is removed via ion exchange with the excess anion present in solution. A basic tenet of this plausible mechanism is that ion exchange between the clay and the solution is much easier when monovalent ions are involved. It could even be argued that the conversion of the interlayer carbonate ions into monovalent ions is a prerequisite: It allows the interlayer spacing to increase to allow accommodation of the much larger surfactant molecules. Iyi et al. [90] also observed that a high degree of substitution requires the presence of a large excess of the counterion in high concentration (>4 mol/L). The ease of substitution also decreases with increase in x, the fractional aluminum substitution in the layers. These two factors may explain why only partial replacement of carbonate was achieved in the present study.

Conclusions

Direct intercalation of surfactants in LDH–CO_3 is difficult owing to the tenacity by which the carbonate is held. The regeneration method has been used successfully to replace carbonate with other guest ions. In this method the LDH–CO_3 is heated and converted into an essentially carbonate-free layered double oxide. This product is then suspended and stirred in aqueous medium containing the desired anion. This study showed that, while the method works for dodecylbenzenesulfonate (DBS), problems are encountered when applying it to dodecyl sulfate (DS). The latter surfactant tends to hydrolyze in highly basic medium to form sulfate ions and dodecanol. Thus, LDH–DS prepared by the regeneration method contains LDH–SO_4 as an impurity. Furthermore, the liberated dodecanol may co-intercalate with DS in a bilayer format to give an additional impurity phase. These insights provide explanations for the anomalous pH effect on the d-spacing reported for LDH–DS by other investigations.

Iyi et al. [90, 91] showed that the conversion of LDH–CO_3 into LDH-A, where A is another inorganic anion, is facilitated by the presence of dilute acids as decarbonation aids. It this study this approach was extended to the intercalation of LDH–CO_3 with DS and DBS. It was found that the intercalation proceeded smoothly under mild conditions of pH and temperature when water soluble carboxylic acids were added to aqueous suspensions LDH–CO_3 and surfactant. Compared to the regeneration approach, well-crystallized products with improved purity were obtained. However, the degree of carbonate substitution that was achieved did not exceed 50%. It is well established that much purer products can be obtained using (i) direct synthesis by coprecipitation or (ii) ion exchange starting with LDH–Cl or LDH–, i.e., LDH precursors with more easily exchangeable monovalent anions, e.g., Cl^- or $\text{NO}_3{}^-$. These latter methods should be considered when high purity LDH–DS or LDH–DBS are sought.

Acknowledgements The authors thank Mrs. C. Harnisch of the Leibniz-Institut für Polymerforschung, Dresden e.V. for the Py/GC/MS analysis. Financial support for this research, from the Institutional Research Development Programme (IRDP), the South African Cooperation Fund for Scientific and Technological Developments (NEPAD), the THRIP program of the Department of Trade and Industry and the National Research Foundation of South Africa, as well as Xyris Technology CC, is gratefully acknowledged.

References

1. Brindley GW, Kikkawa S (1979) Am Mineral 64:836
2. Miyata S (1980) Clays Clay Miner 28:50. doi:10.1346/CCMN.1980.0280107
3. Kopka H, Beneke K, Lagaly G (1988) J Colloid Interface Sci 123:427. doi:10.1016/0021-9797(88)90263-9
4. Reichle WT (1986) Chemtech 16:58
5. Jones W, Chibwe M (1990) In: Mitchell IV (eds) Pillared layered structure: current trends and applications. Elsevier, London, p 67
6. Cavani F, Trifirò F, Vaccari A (1991) Catal Today 11:173. doi:10.1016/0920-5861(91)80068-K
7. Miyata S, Kumura T (1973) Chem Lett 843. doi:10.1246/cl.1973.843
8. Kanoh T, Shichi T, Takagi K (1999) Chem Lett 17. doi:10.1246/cl.1999.117
9. Itoh T, Ohta N, Shichi T, Yui T, Takagi K (2003) Langmuir 19:9120. doi:10.1021/la0302448
10. Xu ZP, Braterman PS (2003) J Mater Chem 13:268. doi:10.1039/b207540g
11. Smyth JR, Bish DL (1988) Crystal structures and cation sites of rock forming minerals. Allen and Unwin, London, p 69
12. Bellotto M, Rebours B, Clause O, Lynch L (1996) J Phys Chem 100:8527. doi:10.1021/jp960039j
13. Porter MR (1994) Handbook of surfactants, 2nd edn. Chapman and Hall
14. Tadros TF (2005) Applied surfactants principles and applications. Wiley-VCH Verlag GmbH and Co., Heppenheim, p 53
15. Crepaldi EL, Pavan PC, Tronto J, Cardoso LP, Valim JB (2002) J Colloid Interface Sci 248:429. doi:10.1006/jcis.2002.8214
16. Harwell JH, Hoskins JC, Schechter RS, Wade WH (1985) Langmuir 1:251. doi:10.1021/la00062a013
17. Bitting D, Harwell JH (1987) Langmuir 3:500
18. Chandler D (2005) Nature 437:640. doi:10.1038/nature04162
19. Whitesides GM, Mathias JP, Seto CT (1991) Science 254:1312. doi:10.1126/science.1962191
20. O'Hare D (1991) In: Bruce DW, O'Hare D (eds) Inorganic materials. Wiley, New York, p 167
21. Pavan PC, Crepaldi EL, Valim JB (2000) J Colloid Interface Sci 229:346. doi:10.1006/jcis.2000.7031
22. Dèkány I, Haraszti T (1996) Colloid Surf A 123–124:391. doi:10.1016/S0927-7757(96)03804-6
23. Pavan PC, Gomes GA, Valim JB (1998) Microporous Mesoporous Mater 21:659. doi:10.1016/S1387-1811(98)00054-7
24. Pavan PC, Crepaldi EL, Gomes GA, Valim JB (1999) Colloid Surf A 154:399. doi:10.1016/S0927-7757(98)00847-4
25. Ulibarri MA, Pavlovic I, Barriga C, Hermosín MC, Cornejo J (2001) Appl Clay Sci 18:17. doi:10.1016/S0169-1317(00)00026-0
26. Anbarasan R, Lee WD, Im SS (2005) Bull Mater Sci 28:145. doi:10.1007/BF02704234
27. Colvin VL, Goldstein AN, Alivisatos AP (1992) J Am Chem Soc 114:5221. doi:10.1021/ja00039a038
28. Fendler JH, Meldrum FC (1995) Adv Mater 7:607. doi:10.1002/adma.19950070703
29. Messersmith PB, Stupp SI (1995) Chem Mater 7:454. doi:10.1021/cm00051a004
30. Dèkány I, Berger F, Imrik K, Lagaly G (1997) Colloid Polym Sci 275:681
31. Clearfield A, Kieke M, Kwan J, Colon JL, Wang RC (1991) J Incl Phenom Mol Recognit Chem 11:361. doi:10.1007/BF01041414
32. Labajos FM, Rives V, Ulibarri MA (1992) J Mater Sci 27:1546. doi:10.1007/BF00542916
33. Kloprogge JT, Hickey L, Frost RL (2002) J Mater Sci Lett 21:603. doi:10.1023/A:1015655018529
34. Takagi K, Sichi T, Usami H, Sawaki Y (1993) J Am Chem Soc 115:4339. doi:10.1021/ja00063a060
35. Yang K, Zhu L, Xing B (2007) Environ Pollut 145:571. doi:10.1016/j.envpol.2006.04.024
36. Meyn M, Beneke K, Lagaly G (1990) Inorg Chem 29:5201
37. You Y, Zhao H, Vance GF (2002) Colloids Surf A Physicochem Eng Aspects 205:161. doi:10.1016/S0927-7757(01)01137-2
38. Zhao H, Nagy KL (2004) J Colloid Interface Sci 274:613. doi:10.1016/j.jcis.2004.03.055
39. Xu ZP, Braterman PS (2007) J Phys Chem 13:268
40. Pesic L, Salipurovic S, Markovic V, Vucelic D, Kagunya W, Jones W (1992) J Mater Chem 2:1069. doi:10.1039/jm9920201069
41. Newman SP, Jones W (1998a) N J Chem 22:105. doi:10.1039/a708319j
42. Drezdzon MA (1988) Inorg Chem 27:4628. doi:10.1021/ic00298a024
43. Trujillano R, Holgado MJ, González JL, Rives V (2005) Solid State Sci 7:931. doi:10.1016/j.solidstatesciences.2005.03.003
44. Hussein MZB, Zainal Z, Ming CY (2000) J Mater Sci Lett 19:879. doi:10.1023/A:1006745716997
45. Crepaldi EL, Pavan PC, Valim JB (1999) Chem Commun (Camb) 155. doi:10.1039/a808567f
46. Miyata S (1983) Clays Clay Miner 31:305. doi:10.1346/CCMN.1983.0310409
47. Boehm H-P, Steinle J, Vieweger C (1977) Angew Chem 89:259. doi:10.1002/ange.19770890416
48. Crepaldi EL, Pavan PC, Valim JB (2000) J Mater Chem 10:1337. doi:10.1039/a909436i
49. Venugopal BR, Shivakumara G, Rajamathi M (2006) J Colloid Interface Sci 32:141
50. You Y, Zhao H, Vance GF (2002) J Mater Chem 12:907. doi:10.1039/b106811c
51. Dimotakis ED, Pinnavaia TJ (1990) Inorg Chem 29:2393. doi:10.1021/ic00338a001
52. Miyata S, Okada A (1977) Clays Clay Miner 25:14. doi:10.1346/CCMN.1977.0250103
53. Sato T, Mikako T, Endo T, Shimada M (1987) J Chem Technol Biotechnol 39:275
54. Chibwe K, Jones W (1989) J Chem Soc Chem Commun 926. doi:10.1039/c39890000926
55. Chen W, Qu B (2003) Chem Mater 15:3208. doi:10.1021/cm030044h
56. Bouraada M, Lafjah M, Ouali MS, de Menorval LC (2008) J Hazard Mater 153:911. doi:10.1016/j.jhazmat.2007.09.076
57. Costa FR, Leuteritz A, Wagenknecht U, Jehnichen D, Häußler L, Heinrich G (2008) Appl Clay Sci 38:153. doi:10.1016/j.clay.2007.03.006
58. Hansen HCB, Taylor RM (1991) Clay Miner 26:311. doi:10.1180/claymin.1991.026.3.02
59. Carlino S, Hudson MJ (1994) J Mater Chem 4:99. doi:10.1039/jm9940400099
60. Carlino S, Hudson MJ, Husain SW, Knowles JA (1996) Solid State Ionics 84:117. doi:10.1016/S0167-2738(96)83014-1
61. Nhlapo N, Motumi T, Landman E, Verryn SMC, Focke WW (2008) J Mater Sci 43:1033. doi:10.1007/s10853-007-2251-0
62. Anbarasan R, Lee WD, Im SS (2008) J Serb Chem Soc 73:321. doi:10.2298/JSC0803321A
63. Vaccari A (1998) Catal Today 41:53. doi:10.1016/S0920-5861(98)00038-8
64. Evans DG, Duan X (2006) Chem Commun (Camb) 485. doi:10.1039/b510313b
65. Khan AI, O'Hare D (2002) J Mater Chem 12:3191. doi:10.1039/b204076j
66. Leroux F, Besse J-P (2001) Chem Mater 13:3507. doi:10.1021/cm0110268

67. Fischer H (2003) Mater Sci Eng C 23:763. doi:10.1016/j.msec.2003.09.148
68. Costa FR, Abdel-Goad M, Wagenknecht U, Heinrich G (2005) Polymer (Guildf) 46:4447. doi:10.1016/j.polymer.2005.02.027
69. Costa FR, Wagenknecht U, Jehnichen U, Abdel-Goad M, Heinrich G (2006) Polymer (Guildf) 47:1649. doi:10.1016/j.polymer.2005.12.011
70. Wang B, Zhang H, Evans DG, Duan X (2005) J Mater Chem Phys 92:190. doi:10.1016/j.matchemphys.2005.01.013
71. Choy J-H, Kwak S-Y, Park J-S, Jeong Y-J, Portier J (1999) J Am Chem Soc 121:1399. doi:10.1021/ja981823f
72. Carlino S, Hudson MJ (1995) J Mater Chem 5:1433. doi:10.1039/jm9950501433
73. Adachi-Pagano M, Forano C, Besse J-P (2000) Chem Commun (Camb) 91. doi:10.1039/a908251d
74. Reichle WT (1985) J Catal 94:547. doi:10.1016/0021-9517(85)90219-2
75. Rey F, Fornés V, Rojo JM (1992) J Chem Soc Faraday Trans 88:2233. doi:10.1039/ft9928802233
76. Frost RL, Ding Z, Martens WN, Kloprogge JT (2003) J Therm Anal Calorim 71:429. doi:10.1023/A:1022835305846
77. Kandare E, Hossenlopp JM (2006) Inorg Chem 45:3766. doi:10.1021/ic060071k
78. Coates J (2000) In: Meyer RA (ed) Encyclopedia of analytical chemistry. Wiley, Chichester, p 10815
79. Perez-Ramirez J, Mul G, Kapteijn F, Moulijn JA (2001) J Mater Sci 11:821
80. Kloprogge JT, Frost RL (1999) Phys Chem Chem Phys 1:1641. doi:10.1039/a808496c
81. Kloprogge JT, Frost RL (2000) Appl Catal A 204:269. doi:10.1016/S0926-860X(00)00697-9
82. Rajamathi JT, Ravishankar N, Rajamathi M (2005) Solid State Sci 7:195. doi:10.1016/j.solidstatesciences.2004.10.034
83. Nakagaki M, Yokoyama S (1985) J Pharm Sci 74:1047
84. Bethell D, Fessey RE, Namwindwa E, Robetrts DW (2001) J Chem Soc Perkin Trans 2:1489. doi:10.1039/b102957f
85. Angarska JK, Tachev KD, Kralchevsky PA, Mehreteab A, Broze G (1998) J Colloid Interface Sci 200:31. doi:10.1006/jcis.1997.5334
86. Crepaldi EL, Tronto J, Cardoso LP, Valim JB (2002) Colloid Surf A 211:103. doi:10.1016/S0927-7757(02)00233-9
87. Parker ML, Milestone NB, Newman RH (1995) Ind Eng Chem Res 34:1196. doi:10.1021/ie00043a023
88. Bontchev RP, Liu S, Krumhansl JL, Voigt J, Nenoff TM (2003) Chem Mater 15:3669. doi:10.1021/cm034231r
89. Bish DL (1980) Bull Mineral (Paris) 103:170
90. Iyi N, Matsumoto T, Kaneko Y, Kitamura K (2004) Chem Mater 16:2926. doi:10.1021/cm049579g
91. Iyi N, Okamoto K, Kaneko Y, Matsumoto T (2005) Chem Lett 34:932. doi:10.1246/cl.2005.932
92. Jobbágy M, Regazoni AE (2004) J Colloid Interface Sci 275:345. doi:10.1016/j.jcis.2004.01.082
93. Hu G, O'Hare D (2005) J Am Chem Soc 127:17808. doi:10.1021/ja0549392